1483

MR imaging simulator and optimized multi-echo z-shimmed sequence for temperature mapping near metallic ablation probes

Megan E Poorman[1,2], Yue Chen[3], Robert J Webster III[3,4], Eric J Barth[3], and William A Grissom[1,2]

[1]Department of Biomedical Engineering, Vanderbilt University, Nashville, TN, United States, [2]Vanderbilt University Institute of Imaging Science, Nashville, TN, United States, [3]Department of Mechanical Engineering, Vanderbilt University, Nashville, TN, United States, [4]Department of Neurological Surgery, Vanderbilt University, Nashville, TN, United States

Synopsis

Signal loss near metallic ablation probes can prevent quality MR thermometry guidance of treatment. Previously we proposed an orientation-independent multi-echo Z-shimmed sequence that could recover the lost signal and improve temperature precision near the probe. However, this method was not feasible for online implementation due to the need to acquire high resolution off-resonance maps around the ablator followed by a computationally-intensive optimization. Here we present an MR imaging simulator that calculates images near metallic ablation probes and successfully use it for offline optimization of the multi-echo Z-shimmed pulse sequence.

Purpose

The magnetic susceptibility of metallic ablation probes causes large signal voids that prevent precise MR thermometry near the probes. This is especially a problem when the target lesion is small, such as for RF ablation of the hippocampus to treat epilepsy[1]. Previously, we proposed an orientation-independent multi-echo Z-shimmed sequence that recovered near-probe signal for more precise temperature mapping[2,3]. However, this method was hindered by the need to acquire high resolution off-resonance maps around the ablator and perform computationally-intensive optimization of the -shim gradient moments prior to heating. Here we present an MR imaging simulator that calculates images near metallic ablation probes and use it for offline optimization of a multi-echo Z-shimmed pulse sequence. The simulated images and optimized sequence were validated in experiments using a nitinol RF ablation probe.

Methods

MR image simulation near metallic ablators:

A MATLAB-based tool was developed to simulate the expected field distortion caused by an ablation probe at a given orientation within the magnetic field. A fast Fourier transform method[4] was used to compute the expected off-resonance from the probe based on its magnetic susceptibility and orientation with respect to B_0. This 3D off-resonance volume was input to the image simulation which models RF excitation and refocusing gradients in a 6-echo thermometry sequence at 3 Tesla (slice = 4 mm, TE = 1.5 to 11.5 ms). Z-shimming was implemented by setting the slice refocusing gradient area before each echo to p% of the full refocusing gradient area (Figure 1). Temperature SNR (tSNR) was computed from the simulated images as

$$tSNR \propto T_E e^{\frac{-T_E}{T_2^*}} \int e^{-i\Delta B}$$

where ΔB is the total through-slice phase gradient caused by the susceptibility mismatch and the applied Z-shim. The simulation tool was validated by imaging agar phantoms (1% w/v) with a spherical air void or a 1 mm diameter nitinol ablation probe oriented 0°, 45°, and 90° with respect to B_0.

Optimizing the Z-shimmed gradients in simulation:

The validated simulator was used to select the optimal refocusing scheme that would maximize tSNR across probe and slice orientations. Specifically, the 1mm nitinol ablation probe was simulated within an aqueous volume oriented at 15°steps between

Figures

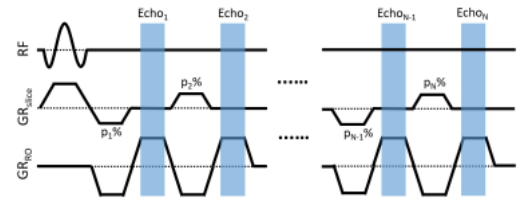

Figure 1: Pulse sequence diagram for the multiple-echo Z-shimmed sequence. Each echo was shimmed separately in the slice dimension by a percentage, *p*, of the full refocusing gradient area. For this application, gradient areas were allowed to vary between 0% and 200% of the full refocusing gradient area.

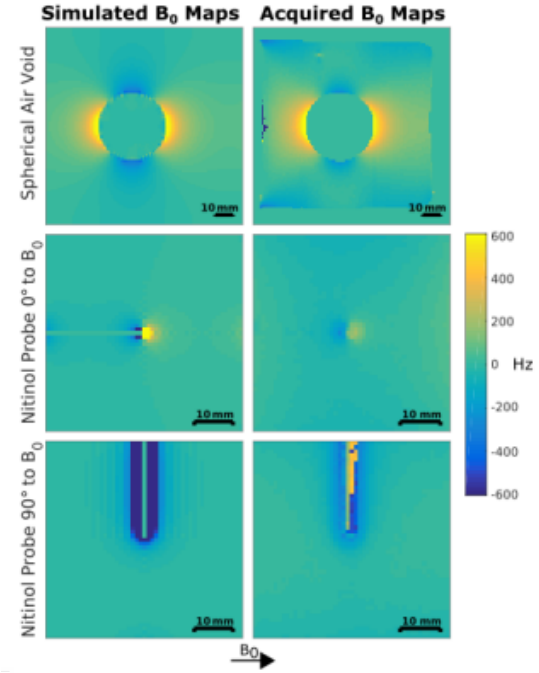

Figure 2: (Left) Field maps simulated using the developed tool for a spherical air void (40 mm Φ) and a nitinol ablation probe (1 mm Φ) at two orientations within the magnetic field. (Right) Acquired field maps of the objects in a 3T scanner (ΔTE = 1ms, Philips Achieva). High order field variations

0°to 90° with respect to B_0. A set of feasible Z-shimmed gradient schemes within 200% of the full refocusing gradient area were generated and applied to the simulation[2]. Images were generated parallel and perpendicular to the probe and used to assess near-probe signal recovery and tSNR for every feasible scheme and probe and slice angulation. For each refocusing scheme tested the tSNR from each orientation was normalized and averaged over the near-probe region. The tSNR was then summed across all orientations and the scheme resulting in maximal tSNR overall was chosen for implementation.

RF ablation with optimized Z-shimmed thermometry:

The optimized refocusing scheme was used for temperature mapping near an MR-compatible, robotic RF ablation system designed for hippocampal ablation[1]. Z-shimmed images were acquired at room temperature for 100 dynamics parallel and perpendicular to the ablation probe and compared to images obtained with a conventional single gradient echo sequence without Z-shimming. A further 100 dynamics were acquired with both the conventional and optimized Z-shimmed sequence immediately following heating with the ablation device. Temperature maps were computed from all image sets using hybrid multi-echo thermometry[5] and compared in terms of temperature precision near the probe.

Results

The simulated field distortions are well correlated with the acquired maps with orientation-dependent field distortions occurring near the embedded object (Figure 2). Images of the nitinol ablation probe generated from the simulated field maps accurately represent the loss of near-probe signal, with the shape and size varying according to probe and slice direction (Figure 3). The optimized Z-shimmed refocusing scheme of p = 200, 20, 180, 60, 140, and 100% (equivalent to phase gradients of -1.3, +1.2, -1.1, +0.8, -0.5, and +0.3 cycles/cm) successfully recovered near-probe signal with up to 5.2 times improvement over the non-Z-shimmed sequence (Figure 4). Temperature precision was improved across all orientations, with the optimized Z-shimmed sequence reducing near-probe variations by 40% on average (Figure 5). A reduction in temperature variation with the optimized sequence was also observed during the heating experiments (results not shown).

Discussion and Conclusions

The optimized Z-shimmed sequence improved near-probe signal recovery and temperature precision for all probe and slice orientations over the conventional thermometry sequence. The validated simulation tool allowed the Z-shimmed sequence to be optimized entirely offline prior to acquisition at the scanner. Future work will explore the use of a look-up table for improved signal recovery and will evaluate its performance compared to the orientation-independent optimized scheme.

Acknowledgements

The authors would like to thank Saikat Sengupta for his help in evaluating the magnetic compatibility of the robotic ablation system. This work was supported by NIH Grants R21NS091735 and T32EB021937.

References

1. Chen Y, Poorman ME, Comber DB, Pitt EB, Liu C, Godage IS, Yu H, Grissom WA, Barth EJ and Webster RJ. Treating Epilepsy via Thermal Ablation: Initial Experiments With an MRI-Guided Concentric Tube Robot. Design of Medical Devices Conference. American Society of Mechanical Engineers 2017.

2. Poorman ME, Grissom WA. Orientation-independent Z-shimmed temperature mapping near ablation probes. Proc. Intl. Soc. Magn. Res. Med. 25 (2017)

3. Zhang Y, Poorman ME, Grissom WA. Dual-Echo Z-Shimmed Proton Resonance Frequency-Shift Magnetic Resonance Thermometry Near Metallic Ablation Probes: Technique and Temperature Precision. Magnetic Resonance in Medicine (Early View) 2017

4. Salomir R, De Senneville BD, Moonen CT. A fast calculation method for magnetic field inhomogeneity due to an arbitrary distribution of bulk susceptibility. Concepts in Magnetic Resonance Part B: Magnetic Resonance Engineering. 2003;19(1):26–34.

can be seen near the objects with good correlation between the simulated and acquired maps. The nitinol wire simulation exhibits the highest shifts near the wire which are not seen in the acquired maps due to partial volume effects and low scan resolution.

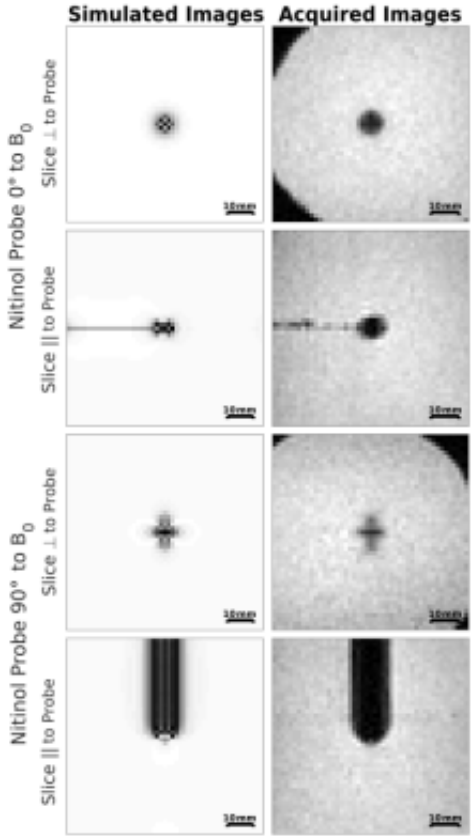

Figure 3: (Left) Images simulated of a nitinol ablation probe (1mm Φ) using the developed tool with no applied Z-shimming. (Right) Gradient echo acquired images of the ablation probe oriented within a 3T scanner (TE = 11.5 ms, TR = 45 ms, Philips Achieva). Signal voids up to 1cm in diameter can be seen near the ablation probe that change shape depending upon probe and slice orientation within the magnetic field. Good correlation in the signal void shape can be seen between the simulated and acquired images.

5. Gaur P, Grissom WA. Comparison of single- and multi- echo PRF-shift thermometry and method of penalized-likelihood multi-echo temperature reconstruction. Proc. Intl. Soc. Mag. Reson. Med. 22(2014) Abstract #2351

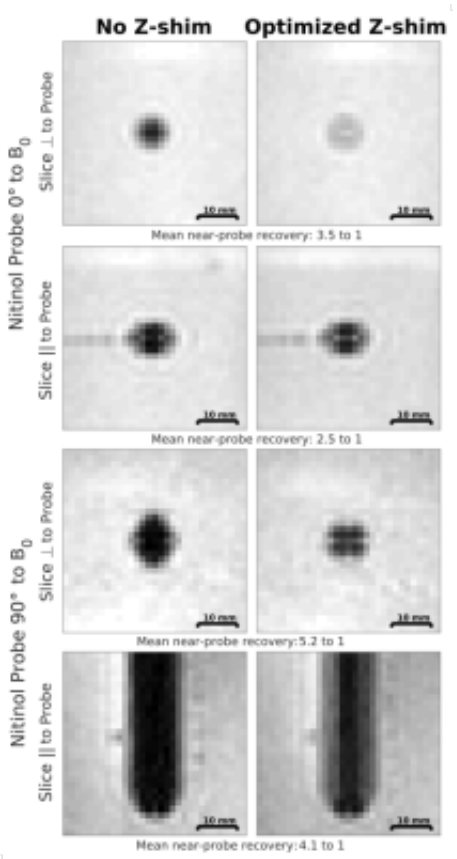

Figure 4: (Left) Conventional gradient echo images without Z-shimming at each probe and slice orientation (TE = 11.5 ms) in a tofu phantom. (Right) Images obtained with the optimized Z-shimmed sequence combined with sum of squares to visualize region of signal loss (TE = 1.5 to 11.5 ms, 6 echoes). Images without Z-shimming exhibit a signal void near-probe approximately 1cm in diameter that is recovered by the optimized Z-shimmed sequence, with up to 5.2 times improvement in near-probe signal.

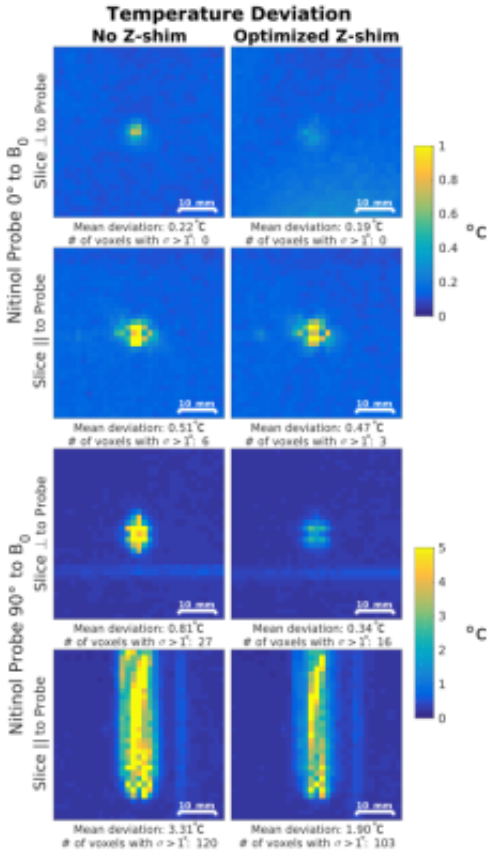

Figure 5: Temperature standard deviation maps at room temperature computed from the conventional gradient echo sequence without Z-shimming (left) and optimized Z-shim sequence (right). 100 dynamics were acquired without heating to observe temperature precision. Average near-probe temperature deviation for each probe and slice orientation is reported below each image. The optimized scheme reduces temperature variation near the probe across all orientation with an overall average reduction in temperature deviation of 40%. The number of pixels with significant standard deviation ($\sigma > 1°C$) was also reduced with z-shimming.